Proceedings World Geothermal Congress 2020+1
Reykjavik, Iceland, April - October 2021

Is the Deep Geothermal Heat Source on Plate Boundaries Affected by Long-term Heat Production and Advection?

Vikram Singh[1*], Benjamin K. Holtzman[2]

[1]Dept. of Chemical Engineering, India Institute of Technology, Delhi, India; [2]Lamont Doherty Earth Observatory, Columbia University, NY, USA

vs225@cornell.edu, benh@ldeo.columbia.edu

Keywords: Geothermal energy source, Crustal thermal structure, Geodynamics

ABSTRACT

Continental plate boundaries provide high potential for geothermal energy production. The thermal structure of plate boundaries is likely to be much more heterogeneous than stable plate interior. Understanding the origins of such heterogeneity will help us assess the geothermal potential as well as seismic hazard. Most models of geotherms on transform plate boundaries assume simple conductive cooling from a mantle adiabat, with possible heat production by fault slip, such as the Lachenbruch and Sass (1980) model applied to the Coast Ranges of California. However, such models may be incomplete and the geothermal potential may be larger than assumed if plate boundaries have both significant viscous dissipation in the strong but aseismic part of the plate boundary (lower crust and upper mantle) in addition to seismic dissipation. Heat produced in plate boundaries may be transferred upwards via conduction and also advection by fluid flow. We consider transform motion of two plates on a boundary of specified width (~10-100 km) driving visco-elastic-plastic deformation in ratios governed by the geotherm and the laboratory derived flow laws, along with hypothetical temperature- and stress-dependent yield stress laws. Viscous deformation is converted into heat continuously. We consider simplified seismic dissipation as a continuous and distributed process over time scales longer than many seismic cycles (averaged over single model time steps of ~ 1e3 yrs), such that the stress is converted to heat where the plate boundary reaches its yield stress. Three observables from the San Andreas plate boundary are compared with the results from the model: average heat flux measured near the surface, estimates of seismic dissipation calculated from average seismicity rates across the entire Coast Ranges, and seismic depth of the brittle-ductile transition estimated roughly from observed earthquake depths. Results indicate that both seismic and viscous dissipation contribute to the heat flux and their ratio significantly depends on the yield stress function used.

1. INTRODUCTION

In this paper, we develop a simplistic model of the thermal-mechanical structure of an active strike-slip plate boundary, in order to explore causes of variability in the geothermal heat source. We examine several basic assumptions commonly made in the calculation of geotherms in the crust and uppermost mantle at plate boundaries, in order to assess the potential for geothermal energy sources in the mid crust in active plate boundaries where there is no volcanic source that is obvious on the surface. While our basic premise is that the heat distribution in the crust is quite heterogeneous, the near-surface geotherm can be effectively dispersed by groundwater flow, e.g. Manga (1998), so may not closely represent the 3D crustal heterogeneity.

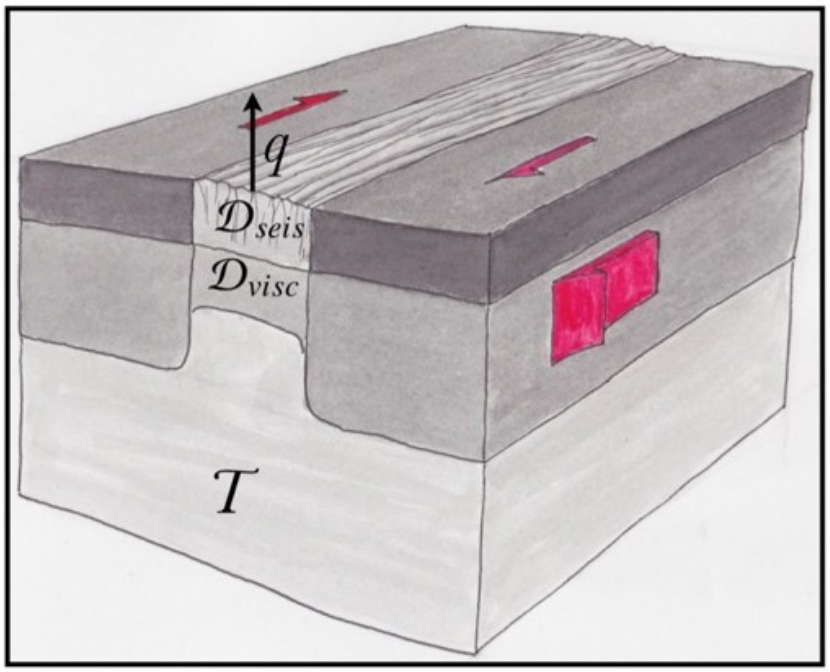

Figure 1. Sketch of plate boundary.

We therefore will construct 1D models of open system heat diffusion and advection through the plate boundaries, where heat sources are only conduction from the convecting mantle, and viscous and frictional dissipation, but no direct magmatic or radioactive, as illustrated in Fig. 1. One aim of the modelling is to get a sense for the broad-brush physics that determine the possible variability in the geothermal source region. For example, what range of temperatures might we expect at 4 km depth, for the range of approximations of physical processes that we explore?

We compare the models initially to three observables (1) the heat flow, as discussed above, (2) the temperature at 4 km depth, an example target reservoir depth, and (3) the seismic dissipation. The seismic dissipation is an elusive number, due to the short nature of our history of collecting seismic data and the many uncertainties in its mathematical definition. A useful way of characterizing the energy balance of a single earthquake is illustrated in Fig 2., after Kanamori and Brodsky (2004). Another not shown here is the depth to the base of the seismogenic zone (including tremor or not). We calculate seismic dissipation rates for the San Andreas using the method in Fig 2, for a range of the uncertainties in the parameters shown in (b) and (c). Obviously, the uncertainties are quite large. Another useful observable diagnostic is the depth to the base of the seismogenic zone, including and excluding tremor and low frequency earthquakes, but that is beyond the scope of the current paper.

2. METHODS

We describe our model below, first in the form of the energy equation, followed by fluid transport properties, and then the pieces of constitutive models that we employ here.

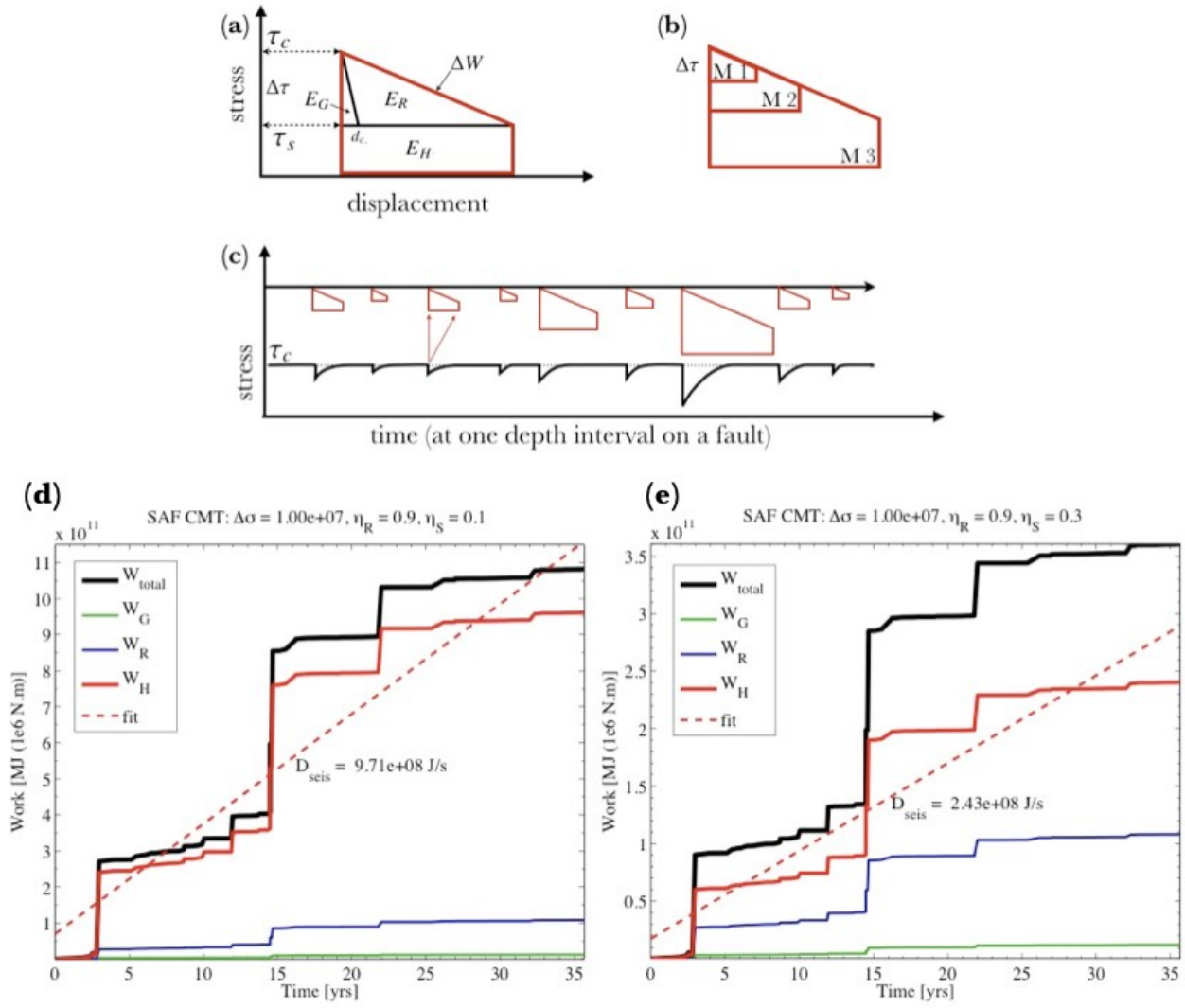

Figure 2. Method for estimating seismic dissipation

2.1 Thermal energy conservation

The classical mode of heat transfer from the mantle to the outer crust is conduction. In the case of a plate boundary, the sliding of tectonic plates can lead to the formation of a porous media where liquid magma can also flow. So, in addition to conduction at the plate boundaries, convection is another potentially important mode of transport. Apart from the flow of heat from the mantle to the outer surface there is also generation of heat inside the plate boundary due to viscous dissipation or due to frictional heating during seismic activities.

A relatively general case for heat transport across a finite thickness of material (i.e. a plate or plate boundary) is the absence of thermal equilibrium between a fluid and solid, in which the fluid is migrating or percolating through the permeable solid. In this case the heat flow through the solid phase and the fluid phase can be written as:

$$(1-\phi)(\rho C)_s \frac{\partial T_s}{\partial t} = (1-\phi)\nabla \cdot \kappa_s \nabla T_s + (1-\phi)\mathcal{D}_s + q_{fs} \quad (1)$$

$$\phi(\rho C)_f \frac{\partial T_f}{\partial t} + (\rho C v)_f \cdot \nabla T_f = \phi \nabla \cdot \kappa_f \nabla T_f + \phi \mathcal{D}_f - q_{fs} \quad (2)$$

where q_{fs} is the heat flow from the fluid phase to the solid phase, ρ is the density of the rock constutiting the REVs throughout plate boundary, C is the heat capacity, T is the temperature, v is the superficial advection velocity of the fluid, κ is the thermal conductivity, and $\mathcal{D}$ is the dissipated mechanical energy per unit volume. Here the subscript s and f refer to the solid and the fluid phase. For a heat transfer coefficient h, $q_{fs}=h(T_f - T_S)$.

The above Eq. 2 can be simplified by assuming that the fluid phase and the solid phase are in local thermal equilibrium, $T = T_f = T_s$:

$$(\rho C)_m \frac{\partial T}{\partial t} = \nabla \cdot \kappa_m \nabla T - (\rho C)_f v \cdot \nabla T + \mathcal{D} \quad (3)$$

The first term on the right-hand side above is the conductive heat transfer, the second is the convective (or advective) heat transfer term and the third is the mechanical heat generation term. All material properties (e.g. $\rho C, \kappa$) are calculated as a weighted sum of fluid and solid values, and given subscript m. The mechanical heat generation this model can be due to viscous dissipation and seismic dissipation. We define these separately below.

2.1.1 Effective fluid transport properties

Rock is generally permeable to fluids through networks of connected pores and fractures. In plate boundaries, to first order, fluid flow is driven upwards by density differences between the fluid and the surrounding rock, as well as by dynamic pressure gradients due to variations in the mean stress or hydraulic head. The velocity of the fluid flowing through the porous media is well described by Darcy's equation:

$$\mathbf{v} = \frac{K \nabla P}{\mu_f} \quad (4)$$

where P is the pressure in the fluid phase, k is the permeability (not to be confused with K, the thermal conductivity), μ_f is the viscosity of the fluid phase, and **v** is the uniform Darcy velocity of the fluid phase across the porous plate boundary (which equals the actual fluid velocity reduced by the porosity, $v = \varphi v_f$).

In the context of this paper and model, we are thinking of this permeability as a large-scale property that is perhaps better called "leakiness". We are ignoring all the physics that control grain scale permeability across a wide range of temperatures, and conditions in which the fluid alters its own pathways and thus permeability, as well as direct coupling between deformation and fluid topology and effective permeability.

Deformation of rock can increase permeability by "damage", a non-specific process term for any deformation-induced change in the internal rock structure, that can often modify the fluid pathways, increasing permeability (for a given porosity). Such processes can include brittle fracture, creep fracture in the presence of fluids (Poulet et. al, 2011) or stress-driven effects on melt distribution at high temperature (e.g. Holtzman et al., 2003). Furthermore, these processes can lead to macroscopic transient processes, such as vug waves (Morgan and Holtzman, 2005), viscous porosity waves (e.g. Speigelman, 1993), visco-plastic porosity waves (Connolly and Podladchikov, 2015), or waves of fluids along faults (e.g. Miller and Nur, 2000). Such transient macroscopic processes will lead to greater volumes of fluid transport than static, microscopic permeability. However, they are not formally described by Darcy's Law.

In this paper, we do not consider these processes explicitly. We reduce these questions to a simple approximation using a notion of an effective permeability in the context of Darcy's law, with that effective permeability as an unknown parameter. Considering that the time steps we use for the following calculations are on the order of 1000 years, we treat this effective permeability as spatially and temporally constant. We consider this leakiness to represent how much heat is advected through the plate by whatever means. It is likely, in nature, that the energy is transferred somewhat indirectly along the path to the surface. For example, basaltic fluid intrudes the lower crust, and starts to partially melt and also to dehydrate aqueous minerals that produce aqueous fluids that then rise upwards, carrying sensible heat and latent heat that will be released when they precipitate new minerals. Over 1000-year time steps, we consider these processes to be relatively smoothly varying. In future work, we will study explicitly the direct coupling with deformation throughout the plate boundary.

2.2 Mechanical energy conservation

Mechanical energy conservation is determined by a constitutive model and momentum conservation. In the version presented here, we consider slow deformation at constant rate in depth and time, so we do not need a momentum equation. However, an emphasis of the model is the contribution of the mechanical energy dissipation to the thermal structure of the plate, in cases where that heat produced remains where it is and cases where it can be advected with a rising fluid. For the case of a deforming plate boundary, the mechanical energy dissipation, $\mathcal{D}$, can be most simply considered to be the sum of two contributions:

$$\mathcal{D} = \mathcal{D}_{seis} + \mathcal{D}_{visc} \quad (5)$$

where $\mathcal{D}_{seis}$ is the energy dissipation due to seismic activities (frictional heating) and $\mathcal{D}_{visc}$ is the viscous energy dissipation per unit volume, which is given by $\mathcal{D}_{visc} = \tau\dot{\gamma}_{visc}$. Here we neglect the heat generation due to radioactivity, as well as the dissipation due to fluid flow. $\mathcal{D}_{seis}$ is energy dissipation during seismic events, given by:

$$\mathcal{D}_{seis} = \begin{cases} 0, & if \quad \tau < \tau_{max} \\ \tau_{max}(\dot{\gamma}_{total} - \dot{\gamma}_{visc}), & if \quad \tau = \tau_{max} \end{cases} \qquad (6)$$

where τ_{max} is the maximum stress sustained by the crust before yielding. Here, the difference between the total strain rate ($\dot{\gamma}_{total}$) and the viscous strain rate ($\dot{\gamma}_{visc}$) is the strain rate due to seismic activity of the plate boundary. We use a depth dependent maximum stress for the current work as described in Section 2.2.2.

$\dot{\gamma}_{visc}$ and $\mathcal{D}_{visc}$ are determined from the constitutive model. As a first approximation, we consider the plate boundary to be a nonlinear Maxwell viscoelastic material. The linear elastic spring and all the irreversible deformation mechanisms are connected in series. We consider two classes of mechanisms: steady state viscous creep and a pressure- and temperature-dependent yield stress. To calculate the amount of viscous dissipation of mechanical energy, we calculate viscous stress and viscous strain rates across the deforming plate. Using a constant strain rate ($\dot{\gamma}_{total}$) across the plate boundary at all depths, for a Maxwell viscoelastic fluid we have, $\dot{\gamma} = \dot{\gamma}_v + \dot{\gamma}_e$, and the Maxwell viscoelastic model:

$$\dot{\gamma} = \frac{\sigma(t)}{\mu_s} + \frac{d\sigma}{Edt} \qquad (7)$$

Stress and strain rates are calculated to convergence in each time step.

2.2.1 Steady state flow laws

At high temperatures in the lower regions of the plate boundary, the empirical flow laws for each deformation mechanism follow the same basic form, e.g. Hirth and Kohlstedt (2003); Hansen et al. (2012), determined for steady-state creep rates.

$$\dot{\varepsilon}_i(\sigma, g, T, P) = A_i^o \sigma^{n_i} g^{-m_i} \exp(-Q_i/RT) = A_i \sigma^{n_i} g^{-m_i} \qquad (8)$$

where i = 1 for diffusion creep, i = 2 for dislocation creep and i = 3 for dislocation- accommodated grain boundary sliding (GBS)creep. Effects of pressure, water content and melt fraction φ are not incorporated in this paper. Parameters values are given in Hansen and Kohlstedt, 2012. Because these processes are considered to act in series, with the total rate limited by the fastest mechanism. Grain size, g, evolves according to a stress- and temperature-dependent piezometer (Austin and Evans, 2007). These flow laws are the same for the crustal and mantle materials. For the crust, we use a wet anorthite flow law from Rybacki et al. (2005).

In the calculation, the transition from crustal composition to mantle composition across the Moho is made gradually, with error functions to weight the contributions of crustal and mantle flow laws using a simple linear combination, across about 10km. Other compositional dependent properties (elastic moduli, heat capacities, etc) are treated the same way. Using an error function, the mantle (Xm) fraction is smoothly varied from 0 to 1 in the transition region. The crustal composition is defined as $Xc = 1 - Xm$.

2.2.2 A peak stress-depth function for seismic deformation

The much more complex and less well understood region in the plate boundary is the transition from steady state creep up to the unstable frictional region where earthquakes occur. Within this transitional region, rocks probably pass through a state of localized deformation due to organized fluid flow and/or grain size reduction localization at some mesoscopic length scale, much larger than the grain size and much smaller than the width of the plate boundary, and then up into a region with transient slip on some time scale (i.e. tremor, slow slip and/or low frequency earthquakes), possibly on previously localized structures (shear zones or faults). Compared to homogeneous creep and frictional instabilities, these transient, transitional processes are not well understood. Here, we propose a simple constitutive model to describe these transitions in a qualitative, time- and space-averaged way. The stress in the plate boundary at any time, $t + 1$ is determined using the following equation:

$$\sigma_{t+1} = \sigma_t + E(\gamma - \gamma_{visc})dt \qquad (9)$$

where E is the elastic modulus, γ is the total strain rate and γ_{visc} is the viscous strain rate determined from the constitutive equation. The stress is allowed to grow to the peak stress where any increase in the stress leads to seismic events.

The standard way to construct a "strength envelope" would be to take Byerlee's law ($\tau = S_0 + \mu(\sigma_n - P_f)$, or

$$\tau = 0.85\sigma_n, \text{for P} < 200 \text{ MPa} \text{ , and } \tau = 50 + 0.6\sigma_n, \text{for P} > 200 \text{ MPa} \qquad (10)$$

People have generally used these rules in combination with steady state flow laws; where they intersect, one chooses the smaller of the two predicted stresses. This approach leads to a pointy "beak" in the strength with very large gradients in stress. These gradients will likely be eliminated by some combination of a wide range of processes including (from top to bottom) brittle/ductile phenomenon that produces slow slip/ tremor, localization of strain by grain size reduction in shear zones, then a transition into homogeneous flow. As a descriptive placeholder for better understanding, we provide a simple function to describe this transition, illustrated in Fig. 3. For that, we propose the following simple function for peak stress, τ_{max}. It has a pressure dependence, using an error function such that it follows Byerlee's law until a certain depth, and then starts to lose its pressure dependence reflecting the closing of cracks and pore spaces by creep (Fig 3b). At about that depth, the linear temperature dependence kicks in and slowly lowers the peak stress (Fig. 3a). First the temperature dependence of the peak stress

$$\tau_{max}^{T} = \tau_{max}^{0}\left(1 - c\frac{(T-T_0)}{T_0}\right) \quad (11)$$

followed by the pressure dependence:

$$\tau_{max} = \tau_{max}^{T}\mathrm{erf}(bP) \quad (12)$$

b and *c* are two parameters that need to be fit. *b* controls how the error function fits with Byerlee's law. *c* controls the temperature sensitivity, and the sign can be positive or negative, depending on whether increasing temperature causes rock toughness to increase (positive) or local creep to lead to overall weakening (negative). These are open questions for different kinds of seismic processes.

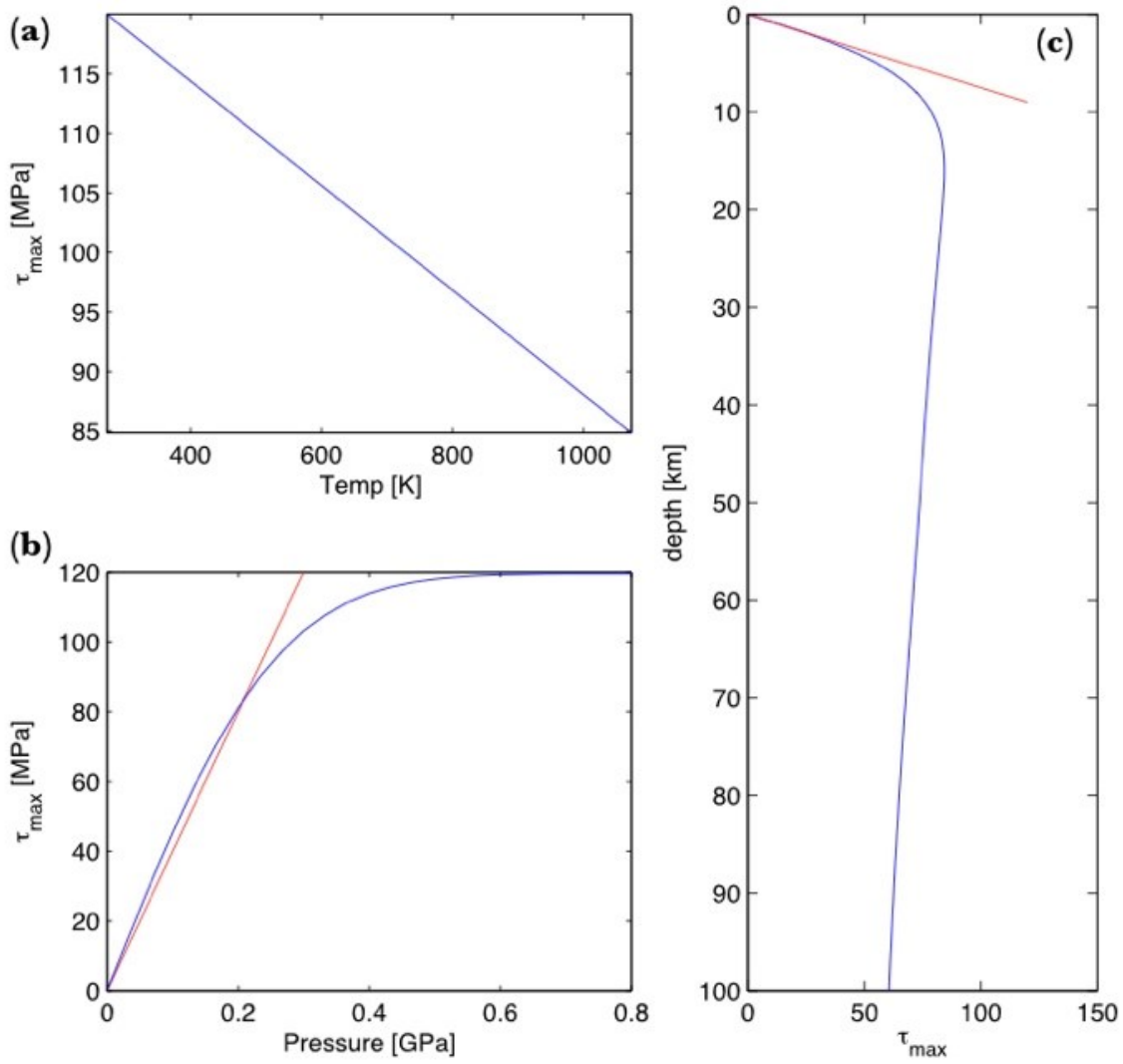

Fig. 3c shows the dependence of maximum stress in the plate boundary on depth.

2.4 Summary of the model

We apply a constant strain rate to a 1D thermal-mechanical structure representing the upper 100 km of a plate boundary. We calculate the seismic dissipation and the viscous dissipation as heat sources in the mantle and crust. The initial condition is a static plate cooling model (not shown). This initial condition represents the non-deforming adjacent continental crust. In one model, we allow the heat to flow only by conduction. In another model, we allow it also to advect, through a constant flux characterized by a long-term effective permeability that we prefer to call "leakiness". These various conditions can be characterized by the Brinkman and Peclet numbers, discussed briefly below. In the model developed here, the plate boundary is considered to be of finite height, *H*, width, *W*, and thickness, *L* where *L* >> *H*, *W*. Due to the large thickness of the plate boundary, the temperature gradients in the horizontal directions (Fig 1) can be neglected. The problem of heat transport across the plate boundary is then reduced to one spatial dimension. We calculate multiple potential observables, but here focus on the heat flow at the surface, the seismic dissipation and the temperature at 4 km, a reasonable geothermal reservoir target depth. The depth to the base of the seismogenic layer is another relatively measurable diagnostic, but is not demonstrated in this paper (yet).

2.4.1 Feedbacks through temperature, stress and grain size

In addition to the feedbacks through deformation, permeability and fluid flow, as discussed above, other feedbacks are accessible through evolution of the grain size and temperature. As the plate boundary deforms, the grain size evolves as a function of temperature, stress and strain rate (i.e. dissipated energy). We use equations of state for grain size, assuming that the rate of change

of grain size is much faster than that of heat flow. In this view, at each time step we assume that the grain size has reached steady state. Two separate steady state grain size models are used for the crust and the mantle in the model. Steady state grain size for the crust is given by Austin and Evans (2008) and modified by Behn et al. (2009). The uniform initial condition for grain size is 5 mm.

Thus, under constant strain rate conditions grain size allows a stabilizing feedback, in that, in certain deformation regimes, as grain size decreases, viscosity decreases so viscous dissipation decreases. Under constant stress conditions, grain size reduction is a positive feedback. Such feedbacks are likely in gravitationally driven faults or boundaries, but transform faults are more likely to be rate limited by distant force balances, such that local weakening could not runaway.

2.4.2 Scaling and Efficiencies

The Peclet number is the ratio of convective (or advective) heat transfer to conductive heat transfer. Higher Peclet number corresponds to higher convective heat transfer compared to conduction. The Peclet number is

$$Pe = \frac{v_d H}{\alpha_f} = \frac{K(dP/dy)}{\mu_f}\frac{H}{\alpha_f} \propto \gamma$$

The Brinkman number is the ratio of dissipative energy generated to energy transported via conduction (References). For the case of a deforming plate boundary there is heat generation due to viscous dissipation and seismic dissipation. Brinkman number is given by:

$$Br = \frac{(\mathcal{D}_{visc} + \mathcal{D}_{seis})H^2}{\kappa T}$$

where H is the depth (or height) of the plate boundary. Higher Brinkman number corresponds to generation of higher dissipative energy.

3. RESULTS

We present a limited set of results here, with the intent to show how sensitive the temperature at 4 km is to the parameters that we vary, namely the peak stress and the leakiness.

3.1 Time series

Fig. 4a shows the near steady state distribution of the energy dissipation. First, it is apparent that the viscous dissipation may be on the same order as the seismic dissipation would be. Allowing advection brings the viscous regime closer to the surface, eroding away from the seismogeneic region. In time, the surface heat flow reaches the measured values in a few million years. Likewise, the seismic dissipation decreases from its early peak, as the grains, heat and viscosity are all decreasing. Both those observables arrive in the bounds of the measurement uncertainty/variablility.

3.2 Steady state observables

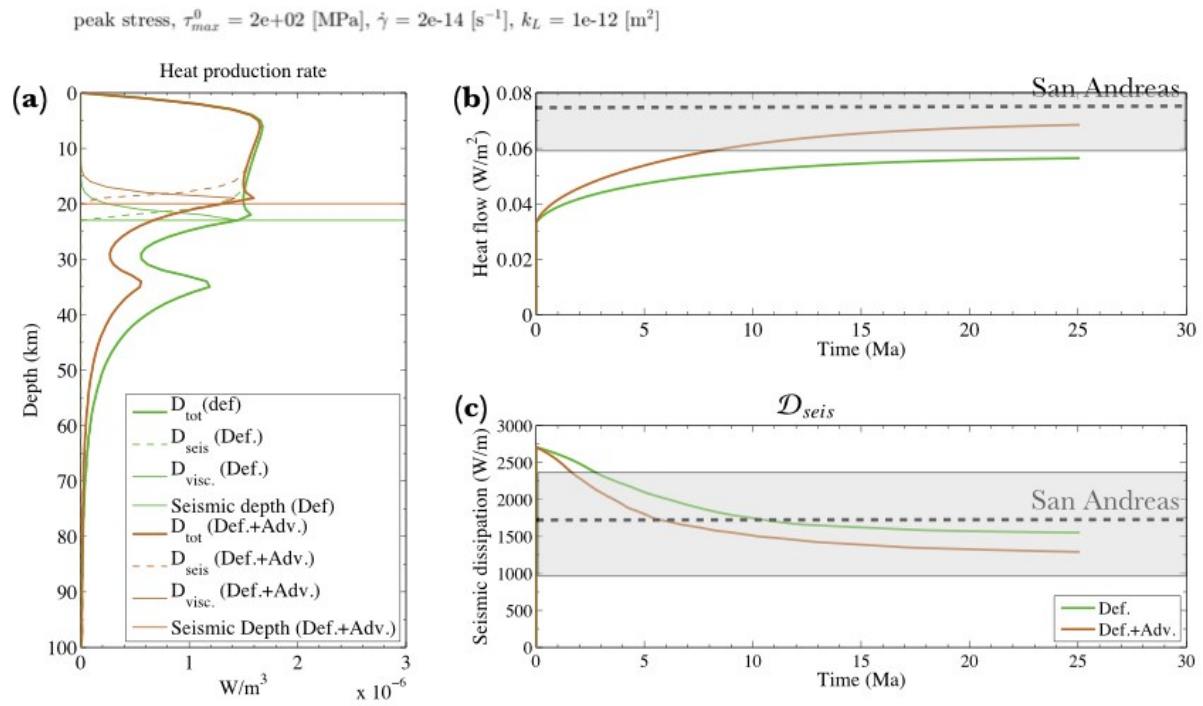

Figure 3. Results, final structure and time series for two runs, with and without heat advection by fluid flow.

In Fig 5, we show predictions for a parameter sweep through leakiness and peak stress parameters. Seismic dissipation increases as the peak stress increases (Fig. 5a), and decreases as the leakiness increases (because the added heat erodes the height of the

seismogenic zone. Similarly, higher peak stresses cause a slight increase in surface heat flux due to increased seismic dissipation, but permeability increases of an order of magnitude, from 1e-11 to 1e1-12 hugely increases the surface heat flux (Fig. 5b) and also the temperature at 4 km (Fig 5c). The seismic dissipation is more sensitive to peak stress, while the thermal structure is more sensitive to leakiness. For increasing/decreasing plate strain rates, these surfaces shift up/down, not shown. From the T@4km plot, it is clear that a wide range of temperatures are possible, based especially on the leakiness (orders of magnitude).

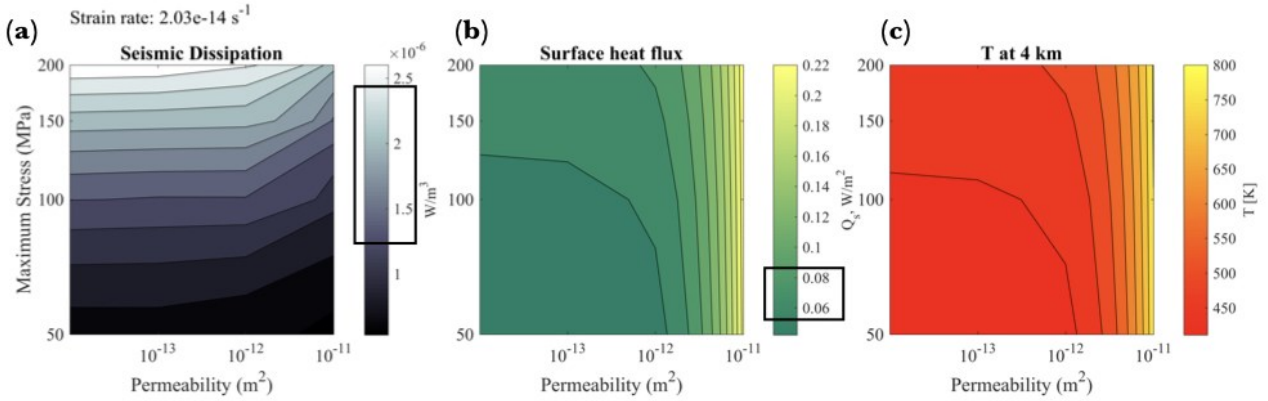

Figure 4. Results at steady state for observables, from multiple runs varying peak stress and permeability (leakiness).

3. CONCLUSIONS AND FURTHER QUESTIONS

We have built a relatively simple plate boundary model to assess the controls and potential variability of the thermal structure, with some fairly significant limitations to the model. Here we return to the question of heterogeneity of the geothermal heat source at 4 km. How much of the heat flow is due to advection of molten rock up to some depth, and how much is due to advection of aqueous fluids? How much of the heat source is conducted from the convecting mantle, dissipated by (seismic or viscous) deformation in the plate boundary or produced by radioactive decay (not studied here)? These questions can be addressed with more analysis of these models, in particular with dimensional analysis comparing Brinkmann and Peclet number. Furthermore, the necessity to develop more sophisticated models seems clear. More richness is warranted in the coupling between the evolving rock structure and the leakiness to fluids of any kind. More realistic definitions of the kinetics and phase equilibria of melt-rock reactions will give more empirical approaches for incorporating approximation of natural complexity.

REFERENCES

Austin, N.J. and Evans, B.: Paleowattmeters: A scaling relation for dynamically recrystallized grain size. *Geology*, 35(4):343–346, 2007

Behn, M. D., Hirth, G., and Elsenbeck II., J. R.: Implications of grain size evolution on the seismic structure of the oceanic upper mantle. *Earth and Planetary Science Letters*, 282:178–189, (2009).

Connolly, J. A. D. and Podladchikov, Y.Y.: An analytical solution for solitary porosity waves: Dynamic permeability and fluidization of nonlinear viscous and viscoplastic rock. *Geofluids* 15(1-2), (2015), 269-292.

Holtzman, B. K., Kohlstedt, D. L., Zimmerman, M. E., Heidelbach, F., Hiraga, T., and Hustoft, J.: Melt segregation and strain partitioning: Implications for seismic anisotropy and mantle flow. *Science*, 301(5637), 1227-1230, (2003).

Hirth, G. and Kohlstedt, D. L.: Rheology of the upper mantle and the mantle wedge: A view from the experimentalists. *Geophysical Monograph American Geophysical Union*, 138:83–105, (2003)

Kanamori, H. and Brodsky, E.: The physics of earthquakes. *Reports on progress in physics,* 67:1429–1496 (2004).

Lachenbruch, A. and J. H. Sass.: Heat flow and energeticso f the san andreasf ault zone. *Journal of geophysical research*, 85(B11), (1980), 6185-6222.

Manga, M.: Advective heat transport by low-temperature discharge in the Oregon Cascades. *Geology,* 26(9), (1998). 799-802.

Miller, S. A., & Nur, A.: Permeability as a toggle switch in fluid-controlled crustal processes. *Earth and Planetary Science Letters*, *183*(1-2), (2000), 133-146.

Morgan, J. P. and Holtzman, B. K.: Vug waves: A mechanism for coupled rock deformation and fluid migration, *Geochemistry, Geophysics, Geosystems,* 6, (2005).

Poulet, T., Regenauer-Lieb, K., & Karrech, A.: A unified multi-scale thermodynamical framework for coupling geomechanical and chemical simulations. *Tectonophysics*, 483(1-2), (2010), 178-189.

Rybacki, E., Gottschalk, M., Wirth, R., & Dresen, G.: Influence of water fugacity and activation volume on the flow properties of fine-grained anorthite aggregates. *Journal of Geophysical Research: Solid Earth*, 111(B3). (2006).

Spiegelman, M.: Flow in deformable porous media. Part 1 Simple analysis. *Journal of Fluid Mechanics*, 247, (1993), 17-38.